



Title	Partitioning Behavior of Mn, Fe, Co, Ni and Zn between an Octahedral Site in Olivine and Silicate Melt
Author(s)	Hashizume, Hideo; Hariya, Yu
Citation	北海道大学理学部紀要, 23(2), 199-209
Issue Date	1992-08
Doc URL	http://hdl.handle.net/2115/36778
Type	bulletin (article)
File Information	23-2_p199-209.pdf



[Instructions for use](#)

PARTITIONING BEHAVIOR OF Mn, Fe, Co, Ni AND Zn BETWEEN AN OCTAHEDRAL SITE IN OLIVINE AND SILICATE MELT

by

Hideo Hashizume* and Yu Hariya**

(with 4 text-figures and 9 tables)

Abstract

Partition coefficients of Mn^{2+} , Fe^{2+} , Co^{2+} , Ni^{2+} and Zn^{2+} between olivine and silicate melt have been determined in the system Mg_2SiO_4 - SiO_2 - H_2O at high pressure and temperature. A partition coefficient is defined by the ratio of the concentration of an element in olivine to that of the element in silicate melt. Olivine has two octahedral sites (M1 and M2 sites). Elements are partitioned among an M1, an M2 sites and silicate melt. We distributed the bulk concentration of the element in olivine to that in the M1 and M2 sites with olivine using the intracrystalline cation distribution data. Partition coefficients between an M1 site and silicate melt, and between an M2 site and silicate melt are shown in a PC-IR (partition coefficient versus ionic radius) diagram. The partition coefficient of Zn^{2+} is exceptionally apart from a linear relationship that those of other elements show.

However, a linear relationship is completed, including the partition coefficient of Zn^{2+} , in a PC-MO (a partition coefficient versus a metal oxygen distance) diagram. M-O distances are the parameter which show the characteristic of both an ionic and a covalent bonding of elements.

Introduction

An element partitioning between minerals and silicate melts has been one of the most fundamental problems in the solid earth sciences. The partition coefficients is strongly affected by temperature and pressure, and, thus, is used to estimate the environment in which an igneous rock has been formed (Takahashi, 1978 *etc.*). The factors, which the partitioning behavior is controlled except temperature and pressure, are the ionic size, crystal field stabilization energy, covalency and electronegativity *etc.*. These factors have been studied by mineralogists and geochemists (Onuma *et al.*, 1968; Henderson and Dale, 1969; Leeman and Scheidegger, 1977; Burns, 1970; *etc.*).

Onuma *et al.* (1968) showed a partition coefficient versus ionic radius (PC-IR) diagram for the first time from the natural andesitic rock system. Partition coefficients of divalent or trivalent cations between pyroxene and groundmass shaped a parabolic curve to ionic radii of divalent or trivalent cations. They proposed that the ionic radii, which positions of peak-tops of the parabolic curve

Contribution from the Department of Geology and Mineralogy, Faculty of Science, Hokkaido University, No. 2066

* National Institute for Research in Inorganic Materials, Tsukuba, 305 Japan.

** Department of Civil Engineering, Hokkaido Institute of Technology, Sapporo, 006 Japan.

showed in the partition coefficient versus ionic radius (PC-IR) diagram, were the best suitable ionic radii in the structure of the relevant mineral. The similar results are shown by Higuchi and Nagasawa (1969), Jensen (1973), Matsui *et al.* (1977), Philpotts (1978), Onuma *et al.* (1981) and Yurimoto and Sueno (1984 & 1987). Matsui *et al.* (1977) mentioned that the partitioning behavior was controlled by the crystal structure. The partition coefficient of Zn^{2+} is not on the parabolic curve in the PC-IR diagram. Matsui *et al.* (1977) and Yurimoto and Sueno (1984) suggested that Zn^{2+} was peculiar cation, and that the deviation of the partition coefficient of Zn^{2+} from the parabolic curve was due to the Zn^{2+} preference of a tetrahedral coordination to an octahedral coordination.

We made a partitioning experiment of divalent cations (Mn^{2+} , Fe^{2+} , Co^{2+} , Ni^{2+} and Zn^{2+}) between olivine and silicate melt. It was attempted to obtain the partition coefficient between an M1 site and silicate melt, and between an M2 site and silicate melt. Further, metal-oxygen (M-O) distances were adopted instead of ionic radii. We proposed the partition coefficients versus M-O distance (PC-MO) diagram and investigated the Zn^{2+} anomaly and the partitioning behavior.

Experimental method

Starting materials were mixtures of MgO, SiO_2 , MnO, CoO, NiO, CuO, ZnO, Fe_2SiO_4 (the synthetic fayalite) and $Mg(OH)_2$ (the synthetic brucite). The compositions of the starting materials (except H_2O) were checked by EDAX (Akashi DS-130+EDAX9100). H_2O content in the starting materials were checked by reducing the sample weight by T.G.. The chemical composition of the starting materials are shown in Table 1.

The high pressure experiment was made by piston-cylinder type apparatus. The pressure transmitting medium was molten pyrex glass. The design of the pressure cell was similar to that figured by Hariya and Kennedy (1968). The sample in the Pt capsule was placed in

Table 1 Chemical compositions of starting materials.

	a	b
MgO	41.2	39.6
SiO_2	43.1	36.8
MnO	1.1	1.1
FeO	1.1	1.1
CoO	1.2	1.2
NiO	2.4	1.8
CuO	3.6	4.1
ZnO	1.8	2.0
H_2O	4.5	12.3
Total	100.0	100.0

Table 2 Experimental conditions and results of high pressure runs.

Run number	starting material	Pressure (GPa)	Temperature ($^{\circ}C$)	Heating time(min)	Results
133	a	1	1400	60	ol, m
307	b	3	1400	88	ol, opx, m

ol; olivine, opx; orthopyroxene, m; silicate melt.

the center of a graphite tube. Pressures were 10 and 30 kbar and a temperature was 1400°C (the temperature difference in the sample is within 10°C). The run duration was about 1 to 1.5 hours (Table 2). We recovered the run products by the quenching method. The part of run products was used for the X-ray powder diffraction and the other part was used for the EPMA analysis.

The chemical compositions of the run products were determined by EPMA (JEOL 733). The analytical conditions for the major elements were different from that for the minor elements, because the content of the minor elements had to be exactly analyzed. Accelerating voltage, beam current and counting time for the peak and back ground were 15 kV, 20 nA, 20 sec and 5 sec for major elements (Mg and Si), respectively. For minor elements (Mn, Fe, Co, Ni, Cu and Zn) accelerating voltage, beam current and counting time for peak and back ground were 25 kV, 28 or 30 nA, 100 sec and 50 sec. The beam diameter was about 3 μm on olivine, and the beam diameter was from 10 to 30 μm on the quenching crystals which showed the melt phase. The number of analysis points was from 30 to 50 points in olivine and the quenching crystals. Walker and Agee (1989) was obeyed on the analytical points.

Result

The average composition of olivine and silicate melt are shown in Table 3. In this paper, the partition coefficient is defined by

$$K_D(X/Mg) = (XO/MgO)^{ol} / (XO/MgO)^m \quad (1),$$

where XO is the concentrations of MnO, FeO, CoO, NiO and ZnO. $(XO/MgO)^{ol}$ and $(XO/MgO)^m$ show the ratios of XO/MgO in olivine and silicate melt, respectively. Error of $K_D(X/Mg)$ is calculated by

$$\delta K_D(X/Mg)^2 = (\delta X/X)_{ol}^2 + (\delta X/X)_m^2 + (\delta Mg/Mg)_{ol}^2 + (\delta Mg/Mg)_m^2 \quad (2),$$

where δX and δMg are the mean error of XO and MgO in olivine and melt, respectively. X and Mg are the averaged composition of XO and MgO in olivine and silicate melt, respectively. $K_D(X/Mg)$ and the mean error calculated from the values in Table 3 are shown in Table 4. Cu was very little concentrations in olivine and silicate melt, so that partitioning of Cu could not be determined in those experiments.

The relationship between the partition coefficient and the ionic radius was shown in Text-fig. 1. This diagram is called as an Onuma or a PC-IR diagram. It showed an almost linear relationship between a partition coefficient and an ionic radius except $K_D(Zn/Mg)$. $K_D(Ni/Mg)$ was the largest and $K_D(Mn/Mg)$ was the smallest of all the partition coefficients. This means that Ni^{2+} is the most concentrated in olivine, and that Mn^{2+} is the most concentrated in silicate melt. That is to say, this shows that the element which has the smaller ionic radius, is concentrated in olivine. $K_D(Zn/Mg)$ was smaller than the partition coefficient estimated from the ionic radius of Zn^{2+} . Zn^{2+} has a different characteristic as compared with other cations on PC-IR diagram (Zn^{2+} anomaly). Matsui *et al.* (1977) and

Table 3 Chemical compositions (wt%) of olivine and coexisting silicate melt.

	Run No. 133				Run No. 307					
	ol.	M. E.	m.	M. E.	ol.	M. E.	m.	M. E.	opx.	M. E.
MgO	50.51	0.13	26.81	3.58	50.87	0.14	35.99	2.30	37.49	0.12
SiO ₂	43.42	0.06	60.93	2.99	43.46	0.22	56.34	1.82	61.22	0.12
MnO	0.36	0.01	0.89	0.05	0.39	0.01	1.33	0.18	0.43	0.02
FeO	0.41	0.02	0.87	0.04	0.46	0.01	0.78	0.09	0.27	0.01
CoO	0.73	0.01	0.55	0.05	0.77	0.01	0.41	0.03	0.33	0.01
NiO	1.88	0.07	0.48	0.07	1.45	0.04	0.21	0.04	0.36	0.03
CuO	0.07	0.01	0.39	0.06	0.02	0.00	0.01	0.00	0.01	0.00
ZnO	1.01	0.02	1.97	0.09	1.24	0.01	2.46	0.35	0.82	0.04
	98.39		92.89		98.66		97.53		100.93	

Atomic ratio (O=4)

	ol.	m.	ol.	m.	opx.*)
Mg	1.8180	0.9637	1.8251	1.2593	0.9311
Si	1.0482	1.4692	1.0461	1.3222	1.0198
Mn	0.0074	0.0182	0.0080	0.0265	0.0061
Fe	0.0083	0.0175	0.0092	0.0153	0.0038
Co	0.0142	0.0106	0.0148	0.0078	0.0044
Ni	0.0366	0.0094	0.0284	0.0040	0.0048
Cu	0.0012	0.0071	0.0003	0.0003	0.0002
Zn	0.0180	0.0352	0.0222	0.0426	0.0101

* oxygen number is 3.

ol.; olivine, m.; silicate melt, opx.; orthopyroxene.

M. E.; mean error.

Yurimoto and Sueno (1984, 1987) suggested that the different characteristic of Zn²⁺ was due to the Zn²⁺ preference of the tetrahedral coordination to the octahedral coordination.

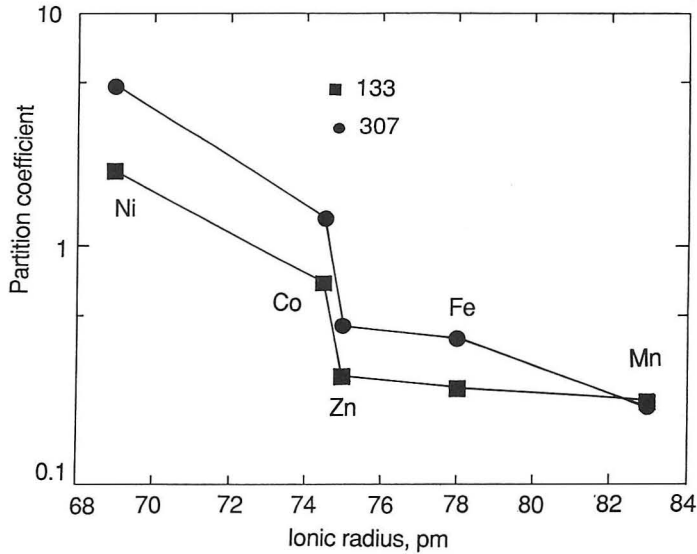
Discussion

PC-IR diagrams of natural basaltic rock and another partitioning experiment between olivine and silicate melt were illustrated in the same figure (Text-fig. 2). The relationship between partition coefficients and ionic radii was almost consistent with each result. In this figure, $K_D(\text{Zn}/\text{Mg})$ was also deviated from the linear relationship. Text-fig. 1 was compared with Text-fig. 2. The PC-IR diagrams were similar to one another, though it is different from the condition in the partitioning behavior.

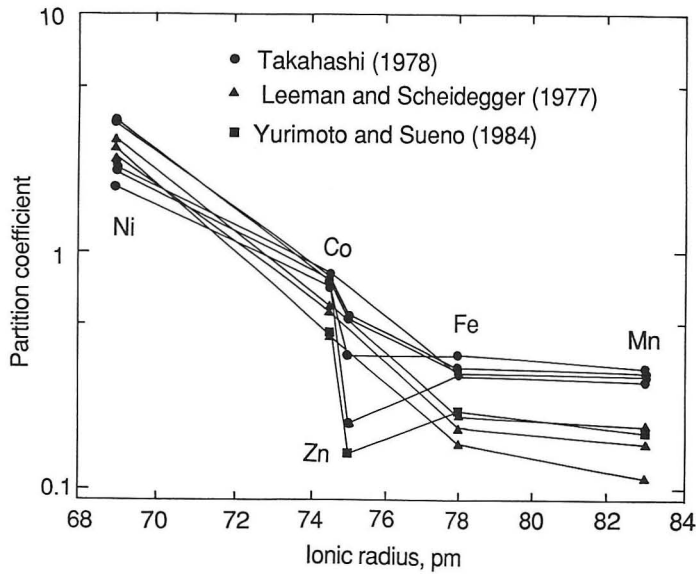
The Zn²⁺ anomaly appeared in PC-IR diagrams (Text-fig. 1 or 2). This can be due to the Zn²⁺ preference of the tetrahedral coordination to the octahedral coordi-

Table 4 Partition coefficients K_D between olivine and silicate melt.

	Run No. 133		Run No. 307	
	K_D	Error	K_D	Error
Mn	0.21	0.22	0.21	0.17
Fe	0.25	0.15	0.42	0.15
Co	0.70	0.16	1.33	0.12
Ni	2.08	0.20	4.89	0.20
Zn	0.27	0.14	0.36	0.16



Text-fig. 1 Partition coefficient-ionic radius diagram for olivine and silicate melt system. Ionic radii data were employed in Shannon and Prewitt (1969).



Text-fig. 2 Partition coefficient-ionic radius diagram for another experimental system and olivine-groundmass system.

nation. However, the electrostatic site energy of Zn^{2+} was compared with that of Mg^{2+} , Fe^{2+} and Mn^{2+} in the regular octahedral site. An element has an energy when the element enters a site. This energy is called the electrostatic site energy. It will become a parameter which shows the degree of the concentration of the

Table 5 Electrostatic site energy (kJ/mol) for Mg^{2+} , Fe^{2+} , Mn^{2+} and Zn^{2+} in octahedral site of carbonates (Smyth & Bish, 1988).

	Site energy
Mg	-255.2
Fe	-253.8
Mn	-241.1
Zn	-253.8

element in a site. The electrostatic site energy of Zn^{2+} was almost same as that of other cations (Table 5). Therefore, it is difficult to explain the Zn^{2+} anomaly only by the preference of the tetrahedral coordination. We would devise the other factors to explain the Zn^{2+} anomaly.

Olivine has two octahedral (an M1 and an M2) sites. An M1 site is almost a regular octahedron and an M2 is a distorted octahedron.

The latter is a larger volume than the former. Therefore, the concentration of a trace element exchanged for Mg^{2+} in the M1 site will be different from that in the M2 site. In this expectation, the Zn^{2+} anomaly will be explained. The concentration of a trace element in olivine is too small to determine it in the M1 and M2 site by the crystal structure analysis. It was attempted to get each concentration of trace elements in an M1 and M2 site, and to obtain a partition coefficient between an M1 site and silicate melt, and between an M2 site and silicate melt.

A distribution coefficient between an M1 and an M2 site is defined by

$$K_D^{M1/M2}(X/Mg) = (A_X^{M1}/A_{Mg}^{M1}) / (A_X^{M2}/A_{Mg}^{M2}) \quad (2),$$

where X is Mn, Fe, Co, Ni, and Zn. A_X^{M1} and A_{Mg}^{M1} are the concentration of XO and MgO in M1 site, respectively. A_X^{M2} and A_{Mg}^{M2} are the concentration of XO and MgO in M2 site, respectively. The chemical composition of olivine is defined by $(Mg_{1-Q}X_Q)_2SiO_4$, and A_X^{M1} is defined by P. Q is the concentration of X in olivine. Then, the other site occupancy ratio are obtained. That is to say, $A_X^{M1} = P$, $A_{Mg}^{M1} = 1 - P$, $A_X^{M2} = 2Q - P$ and $A_{Mg}^{M2} = 1 - 2Q + P$ (Akamatsu *et al.*, 1988). A distribution coefficient $K_D^{M1/M2}(X/Mg)$ is rewritten by

$$K_D^{M1/M2}(X/Mg) = P(1 - 2Q + P) / (1 - P)(2Q - P) \quad (3).$$

We assumed that $K_D^{M1/M2}(X/Mg)$ was constant. The distribution coefficients were employed in Table 6. Q was used for atomic ratios in Table 3. The concentration of a trace element in the M1 and M2 site was calculated. The ratio of the M1 and M2 site of Mg^{2+} was obtained by subtracting the total concentrations of the M1 and M2 site of the trace elements from 1. The concentrations of Mg^{2+} in the M1 and

Table 6 Site occupancy ratios and intracrystalline distribution coefficients for olivines.

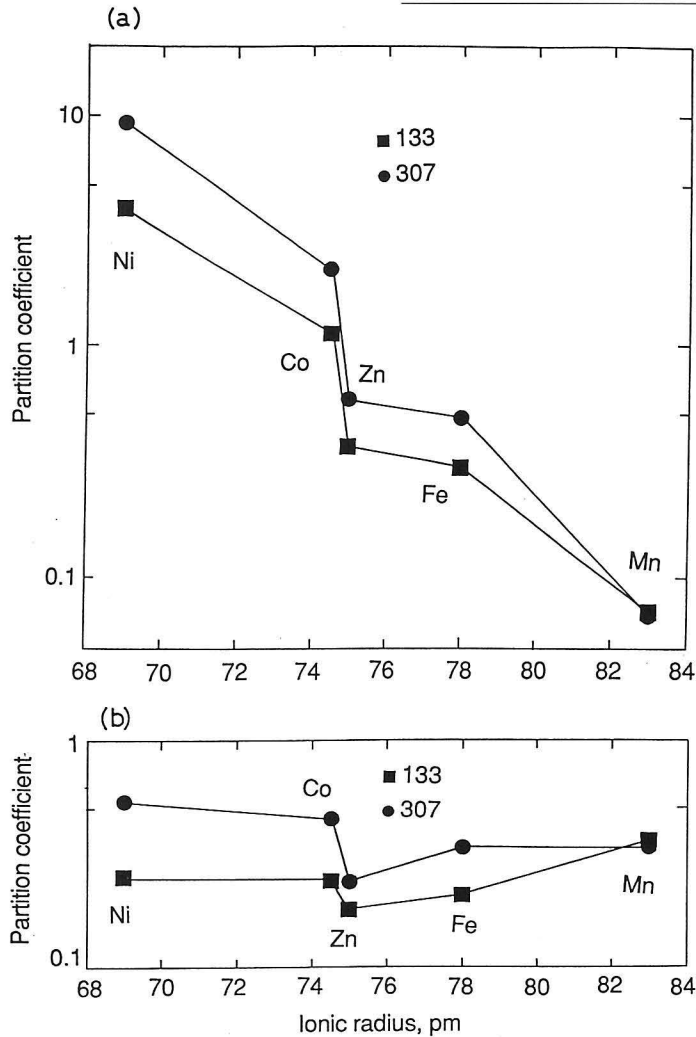
X	M1		M2		$K_D^{M1/M2}$	reference
	X	Mg	X	Mg		
Mn	0.295	0.705	0.685	0.315	0.192	Akamatsu <i>et al.</i> (1988)
Fe	0.077	0.923	0.057	0.943	1.380	Shinno (1980)
Co	0.208	0.792	0.053	0.947	4.693	Miyake <i>et al.</i> (1987)
Ni	0.767	0.233	0.263	0.737	9.225	Rajamani <i>et al.</i> (1975)
Zn	0.273	0.727	0.162	0.838	1.942	Ghose <i>et al.</i> (1975)

Table 7 Site occupancy of an M1 and an M2 site.

	Run No. 133		Run No. 307	
	M1	M2	M1	M2
Mg	0.8994	0.9186	0.9037	0.9214
Mn	0.0012	0.0062	0.0013	0.0067
Fe	0.0048	0.0035	0.0053	0.0039
Co	0.0117	0.0025	0.0122	0.0026
Ni	0.0345	0.0021	0.0268	0.0016
Zn	0.0119	0.0061	0.0146	0.0076

Table 8 Partition coefficients between the M1 site and silicate melt and between the M2 site and silicate melt.

	Run No. 133		Run No. 307	
	$K_D^{M1/11q}$	$K_D^{M2/11q}$	$K_D^{M1/11q}$	$K_D^{M2/11q}$
Mn	0.07	0.36	0.07	0.35
Fe	0.29	0.21	0.48	0.35
Co	1.18	0.25	2.18	0.46
Ni	3.93	0.24	9.34	0.55
Zn	0.36	0.18	0.42	0.24

**Text-fig. 3** (a) Partition coefficient-ionic radius diagram for the M1 site in olivine and silicate melt system. (b) Partition coefficient-ionic radius diagram for the M2 site in olivine and silicate melt system.

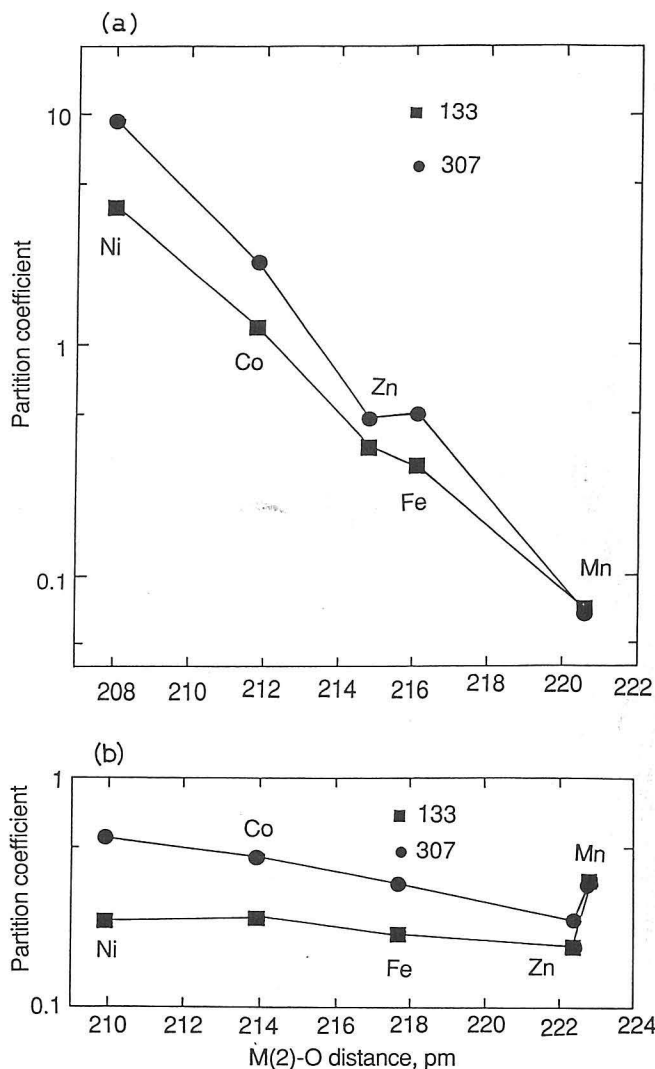
M2 site would be calculated by using the atomic ratio in Table 3 from the ratio of the M1 and M2 sites of Mg^{2+} . The concentrations of Mg^{2+} in the M1 and M2 site was also listed in Table 7. The partition coefficients between the M1 site and silicate melt ($K_D^{M1/m}(X/Mg) = (A_X^{M1}/A_{Mg}^{M1}) / (A_X^m/A_{Mg}^m)$), where A_X^m and A_{Mg}^m are the atomic ratio of X and Mg in silicate melt.) and between the M2 site and silicate melt ($K_D^{M2/m}(X/Mg) = (A_X^{M2}/A_{Mg}^{M2}) / (A_X^m/A_{Mg}^m)$) are shown in Table 8. A_{Mg}^m and A_X^m were used atomic ratio (O=4) of elements in silicate melt in Table 3.

PC-IR diagrams for the M1 site and silicate melt and for the M2 site and silicate melt were shown in Text-fig.3 (a) and (b), respectively. Partition coefficients are almost linearly related to ionic radii. The relationship of partition coefficients between the M1 site and silicate melt to ionic radii are steeper than that of partition coefficients between the M2 site and silicate melt to ionic radii. Therefore, an element, which has a smaller ionic radius, is concentrated in the M1 site. The M2 site is not sensitive on an ionic radius of an element. However, $K_D^{M1/m}(Zn/Mg)$ and $K_D^{M2/m}(Zn/Mg)$ deviate from linear lines. Zn^{2+} anomaly was not explained on the PC-IR diagram.

An ionic radius was determined by an ionic bonding crystal. However, Zn^{2+} in the octahedral site is the cation which has the characteristic of both the ionic and covalent bonding. Therefore, it was unreasonable to explain the partitioning behavior by ionic radii. We propose a metal-oxygen (M-O) distance instead of an ionic radius, because an M-O distance was the parameter which represents both the ionic and covalent bonding. M-O distances (M: Mn, Fe, Co, Ni and Zn) were average values of six distances from the metal to an oxygen in each olivine (Mn_2SiO_4 , Fe_2SiO_4 , Co_2SiO_4 and Ni_2SiO_4) except Zn_2SiO_4 . Zn_2SiO_4 does not build the olivine structure. Therefore, the Zn-O distance of $(Mg_{0.34}Mn_{0.43}Zn_{0.18}Fe_{0.04})_2SiO_4$ (Brown, 1970) was employed. M(1)-O and M(2)-O distances of each olivine were shown in Table 9 (M(1) and M(2) were the metal cation in the M1 and M2 site.). The PC-MO diagrams were illustrated in Text-fig.4 (a) and (b). Partition coefficients were linearly related to M-O distances. For the PC-M(1)O diagram, the element which has a small M-O distance was concentrated in the M1 site as shown in Text-fig 4 (a). Partition coefficients of all elements between the M2 site and silicate melt were similar to each other as shown in Text-fig.4 (b). Therefore, the partition coefficients were not dependent on the M(2)-O distances of the

Table 9 The M(1)-O, M(2)-O and average of M(1)-O and M(2)-O distances (pm) (Avg.) for each olivine.

	M(1)-O	M(2)-O	Avg.	reference
Mn	220.6	222.8	221.7	Fujino <i>et al.</i> (1981)
Fe	216.1	217.7	216.9	Fujino <i>et al.</i> (1981)
Co	211.8	213.9	212.9	Tamada <i>et al.</i> (1983)
Ni	208.0	209.9	209.0	Tamada <i>et al.</i> (1983)
Zn	214.8	222.4	218.6	Brown (1970)



Text-fig. 4 (a) Partition coefficient-M(1)-O distance diagram for the M1 site in olivine and silicate melt system. (b) Partition coefficient-M(2)-O distance diagram for the M2 site in olivine and silicate melt system.

elements. $K_D(\text{Zn}/\text{Mg})$ does not almost represent anomaly for the M1 site and silicate melt system, and for the M2 site and silicate melt system. The Zn^{2+} anomaly in the PC-IR diagram is an apparent anomaly by using the ionic radii. However, the rugged profiles were not represented in the PC-MO diagrams (Text-fig. 4 (a) and (b)). Therefore, we proposed the PC-MO diagram for the investigation of the partitioning behavior instead of the PC-IR diagram.

Conclusion

Elements of Mn^{2+} , Fe^{2+} , Co^{2+} , Ni^{2+} and Zn^{2+} were actually partitioned among an M1 site, an M2 site and silicate melt. We obtained the partition coefficient between the M1 site and silicate melt, and between the M2 site and silicate melt. A partition coefficient of Zn both between the M1 site and silicate melt, and between the M2 site and silicate melt showed the anomalous behavior in the PC-IR diagram (Text-fig. 2 (a) and (b)). However, the partition coefficients were linearly related in M-O distances (Text-fig. 4 (a) and (b)). The Zn^{2+} anomaly did not appear. In investigating the partitioning behavior, we recommended the PC-MO diagram.

Acknowledgements

We would like to thank Assoc. Prof. T. Kikuchi, and Dr. H. Miura of Hokkaido University for their help and encouragements during this work.

References

- Akamatsu, T., Fujino, K., Kumazawa, M., Fujimura, A., Kato, M., Sawamoto, H. and Yamanka, T., 1988. Pressure and temperature dependence of cation distribution in Mg-Mn olivine. *Phys. Chem. Minerals*, 16: 105-113.
- Brown, G. E., 1970. The crystal chemistry of the olivines. Ph. D. Thesis, *Virginia Polytechnic Institute and State University*. Blacksburg, Virginia. pp.1-121.
- Burns, R. G., 1970. *Mineralogical applications of crystal field theory*. Cambridge University Press, England, pp.1-224.
- Fujino, K., Sasaki, S., Takeuchi, Y. and Sadanaga, R., 1981. X-ray determination of electron distributions in forsterite, fayalite and tephroite. *Acta Crystallogr.*, B37: 513-518.
- Ghose, S., Wan, C., Okamura, F. P., Ohashi, H. and Weidner, J. R., 1975. Site preference and crystal chemistry of transition metal ions in pyroxenes and olivines. *Acta Crystallogr.*, A31, Suppl.: S76.
- Hariya, Y. and Kennedy, G. C., 1968. Equilibrium study of anorthite under pressure and high temperature. *Am. Jour. Sci.*, 266: 193-203.
- Higuchi, H. and Nagasawa, H., 1969. Partition of trace elements between rock-forming minerals and the host volcanic rocks. *Earth Planet. Sci. Lett.*, 7: 281-287.
- Jensen, B. B., 1973. Patterns of trace element partitioning. *Geochim. Cosmochim. Acta*, 37: 2227-2242.
- Leeman, W. P. and Scheidegger, K. F., 1977. Olivine/liquid distribution coefficients and a test for crystal-liquid equilibrium. *Earth Planet. Sci. Lett.*, 35: 247-257.
- Matsui, Y., Onuma, N., Nagasawa, H., Higuchi, H. and Banno, S., 1977. Crystal structure control in trace element partition between crystal and magma. *Bull. Soc. Fr. Mineral. Cristallogr.*, 100: 315-324.
- Miyake, M., Nakamura, H., Kojima, H. and Marumo, F., 1987. Cation ordering in Co-Mg olivine solid-solution series. *Am. Mineral.*, 72: 594-598.
- Onuma, N., Higuchi, H., Wakita, H. and Nagasawa, H., 1968. Trace element partition between two pyroxenes and the host lava. *Earth Planet. Sci. Lett.*, 5: 47-51.
- Onuma, N., Ninomiya, S. and Nagasawa, H., 1981. Mineral/groundmass partition coefficients for nepheline, melilite, clinopyroxene and perovskite in melilite-nepheline basalt, Nyiragono, Zaire. *Geochem. J.*, 15: 221-228.
- Philpotts, J. A., 1978. The law of constant rejection. *Geochim. Cosmochim. Acta*, 42: 909-920.
- Rajamani, V., Brown, G. E. and Prewitt, C. T., 1975. Cation ordering in Ni-Mg olivine. *Am. Mineral.*, 60: 292-299.

- Shannon, R. D. and Prewitt, C. T., 1969. Effective ionic radii in oxides and fluorides. *Acta Crystallogr.*, B25: 925-946.
- Shinno, I., 1980. On the distribution of cation in (Mg, Fe)₂SiO₄ solid solution. *Sci. Rep. Dept. Geol. Kyushu Univ.*, 13: 217-224. (in Japanese with English abstract).
- Smyth, J. R. and Bish, D. L., 1988. *Crystal structures and cation sites of the rock-forming minerals*. Boston Allen and Unwin, London, Sydney, Wellington, pp. 1-329.
- Takahashi, E., 1978. Partitioning of Ni²⁺, Co²⁺, Fe²⁺, Mn²⁺ and Mg²⁺ between olivine and silicate melts: compositional dependence of partition coefficient. *Geochim. Cosmochim. Acta*, 42: 1829-1844.
- Tamada, O., Fujino, K. and Sasaki, S., 1983. Structures and electron distributions of α -Co₂SiO₄ and α -Ni₂SiO₄ (olivine structure). *Acta Cryst.*, B39: 692-697.
- Walker, D. and Agee, C., 1989. Partitioning "equilibrium", temperature gradients, and constraints on Earth differentiation. *Earth Planet. Sci. Lett.*, 96: 49-60.
- Yurimoto, H. and Sueno, S., 1984. Anion and cation partitioning between olivine, plagioclase phenocrysts and the host magma: A new application of ion microprobe study. *Geochem. J.*, 18: 85-94.
- Yurimoto, H. and Sueno, S., 1987. Anion and cation partitioning between three pyroxenes, chrom spinel phenocrysts and the host boninite magma: an ion microprobe study. *Geochem. J.*, 21: 85-104.

(Manuscript received on May 28, 1992; and accepted on June 22, 1992)